Pulsed addressing of a dual-frequency nematic liquid crystal

N. J. Mottram[1] and C. V. Brown[2]
[1]*Department of Mathematics, University of Strathclyde, Livingstone Tower, Glasgow G1 1XH, United Kingdom*
[2]*School of Biomedical & Natural Sciences, Nottingham Trent University, Clifton Lane, Nottingham NG11 8NS, United Kingdom*
(Received 14 November 2005; revised manuscript received 19 May 2006; published 11 September 2006)

A continuum theory of dielectric relaxation within liquid crystal materials is described and used to model the response of dual frequency materials to single pulse voltage waveforms. The equations governing the anisotropic axis (director) angle, electric field, and induced polarizations are solved numerically to investigate pulsed addressing of a model zenithally bistable liquid crystal device. By suitably tailoring the voltage pulse, it is found to be possible to switch between both bistable states. For short pulses the high frequency components of the leading edge of the voltage pulse excites the perpendicular polarization and forces the director to lie parallel to the cell substrates. For longer voltage pulses the constant dc component of the voltage pulse excites the parallel polarization causing the director to lie perpendicular to the substrates. It is also found that reducing rotational viscosity and increasing the achievable dielectric anisotropies (particularly the high frequency value) can significantly reduce the operating voltages of such a device.

DOI: 10.1103/PhysRevE.74.031703 PACS number(s): 42.70.Df, 42.79.Kr

I. INTRODUCTION

The dielectric relaxation of liquid crystal materials has been investigated both theoretically [1–4] and experimentally [5,6] over many years. In liquid crystals a bulk polarization can be induced by the application of an electric field via a number of mechanisms, which include the electronic polarization of individual atoms, the electronic polarization of individual molecules, and the reorientation of permanent molecular dipoles. The response of these different polarization mechanisms occurs on different time scales.

The electronic polarization mechanisms exhibit resonant responses to an applied ac electric field. Below this resonant frequency such mechanisms respond to the applied field and contribute to the dielectric susceptibility of the material. For example, at optical frequencies the observed refractive index of many calamitic nematic liquid crystals is enhanced by the electronic molecular polarization mechanism. The anisotropy of the individual nematic molecules, leading to different electronic polarizabilities being exhibited parallel to and perpendicular to the molecular axis, and the tendency for molecules to align parallel to neighboring molecules (creating an average molecular orientation, the "director") then leads to birefringence.

When these materials consist of molecules containing a permanent dipole, bulk polarization may also be induced by partial reorientation of these dipoles to align with an applied field. However, there is a time lag for the reorientation of the dipoles due to the viscosity of the fluid. In Debye theory [1], where it is assumed that the magnitude of the induced polarization evolves exponentially with time, this results in a well defined relaxation frequency, below which the orientational mechanism contributes to the dielectric susceptibility, but above which it does not.

In calamitic nematic liquid crystals a lower relaxation frequency is generally observed when the ac electric field is applied parallel to the director (the average orientation of the molecular long axis) compared to when the field is applied perpendicular to the director. This is because rotation about the short molecular axis is hindered when compared to rotation about the long axis. Typical values are above 10^5 Hz for relaxations in the dielectric susceptibility measured parallel to the director $\chi_{\|}$ and above 10^7 Hz for relaxations in the dielectric susceptibility measured perpendicular to the director $\chi_{\perp}$ [3].

In so called "dual-frequency" or "2f" materials the relaxation in $\chi_{\|}$ occurs at frequencies on the order of 10^3 Hz at room temperature, well below normal values [7,8] so that reasonable voltage addressing schemes may be constructed enabling this relaxation phenomenon to be utilized in a photonic device [8]. At low frequencies well below f_c, the relaxation frequency of $\chi_{\|}$, the dielectric susceptibility anisotropy $\Delta\chi=\chi_{\|}-\chi_{\perp}$ is positive. At frequencies well above f_c the value of $\Delta\chi$ is negative. This effect has previously been exploited for designing voltage addressing schemes to give fast switching in displays [8–10]. However, problems with using dual frequency liquid crystals for this application include a strong temperature dependence of the critical frequency f_c and significant dielectric heating close to f_c. Recently, interest has been renewed in dual frequency nematic materials with the possibility of using them in dual mode display devices [11], as an adaptive element in microwave devices [12], and in phase devices for telecommunication applications [13–15], where accurate temperature control may be possible.

In the present paper we will assume that both electronic polarization effects mentioned above are extremely fast processes with a typical relaxation time on the scale of nanoseconds. We will also neglect any space-charge effects although it is relatively straightforward to include governing equations for positive and negative ion movement within a fluid [16,17].

A number of researchers have investigated theoretical descriptions of dual frequency materials [13,18] although all assume a sinusoidal voltage is applied and therefore a simple empirical frequency dependent dielectric susceptibility anisotropy could be used. In this paper we experimentally determine certain key material parameters needed within a theoretical model of the dielectric relaxation of the liquid

crystal. We then use the Debye approach to describe the time evolution of the polarization due to the reorientation of molecular dipoles parallel to the director. This enables the response of the liquid crystal to arbitrary waveforms to be calculated. Using this theory we consider the pulsed voltage addressing of a zenithally bistable nematic device filled with dual frequency material and show that switching between the two bistable states is possible by tailoring the voltage pulse height and duration.

II. THEORY

The dielectric susceptibility χ of a material relates the bulk polarization per unit volume $\mathbf{P}$ induced in a medium to the applied electric field via $\mathbf{P}=\chi\epsilon_0\mathbf{E}$, where ϵ_0 is the permittivity of free space. The total polarization can be written as the sum of the electronic polarization contributions $\mathbf{P}^e$ produced by a number of mechanisms, and the orientational polarization $\mathbf{P}^o$ so that $\mathbf{P}=\mathbf{P}^e+\mathbf{P}^o$. In a liquid crystal the orientational alignment of molecules creates anisotropy and allows for the definition of an average molecular long axis orientation, the director $\mathbf{n}$. Due to this anisotropy it is necessary to separately consider the induced polarization along the director $\mathbf{P}_\parallel$ and perpendicular to the director $\mathbf{P}_\perp$ as shown in Eqs. (1) and (2).

$$\mathbf{P}_\parallel = \mathbf{P}_\parallel^e + \mathbf{P}_\parallel^o = \chi_{\parallel l}^e \epsilon_0 \mathbf{E}_\parallel + \mathbf{P}_\parallel^o, \tag{1}$$

$$\mathbf{P}_\perp = \mathbf{P}_\perp^e + \mathbf{P}_\perp^o = (\chi_{\perp l}^e + \chi_{\perp l}^o)\epsilon_0 \mathbf{E}_\perp, \tag{2}$$

where $\mathbf{E}_\parallel$ and $\mathbf{E}_\perp$ are the components of the electric field parallel and perpendicular to the director. Since relaxation of the electronic polarization mechanisms is thought to occur well above 10^9 Hz [6] these contributions to the polarization will react at much smaller time scales compared to either the period of any applied oscillating field or the voltage pulse rise time achievable experimentally. The electronic susceptibility values will therefore be considered as remaining constant at their low frequency limits $\chi_{\parallel l}^e$ and $\chi_{\perp l}^e$ as indicated in Eqs. (1) and (2). We will also assume that the relaxation perpendicular to the director also occurs on a time scale that is much shorter than the time scales that we will be considering. This is reasonable assuming this relaxation occurs well into the Megahertz regions, see Ref. [3] and Sec. 5.41 of Ref. [19]. We have therefore taken $\mathbf{P}_\perp^o=\chi_{\perp l}^o\epsilon_0\mathbf{E}_\perp$ in Eq. (2). Relaxation of all these effects can be easily included in the following model using the same method outlined below but this will lead to only minor modifications to the results and significantly increase the computation time.

For the orientational dipole parallel to the director we will assume that any forced response of this polarization obeys a Langevin-type equation, which may be thought of as a resonance free Lorentz equation for dipole relaxation

$$\tau\frac{dP_\parallel^o}{dt} + P_\parallel^o = \gamma E_\parallel, \tag{3}$$

where τ is the relaxation time constant for the parallel orientational polarization $P_\parallel^o$ and γ is the electric field coupling which will be specified in terms of the susceptibility below. For a sinusoidal electric field $E=E_0e^{2\pi ft i}$, the solution to Eq. (3) is readily obtained,

$$P_\parallel^o = \frac{\gamma}{1+2\pi f\tau i}E_\parallel. \tag{4}$$

Using the relationship $P_\parallel^o=\chi_\parallel^o\epsilon_0E_\parallel$ then gives the parallel orientational susceptibility

$$\chi_\parallel^o = \frac{\gamma}{\epsilon_0(1+2\pi f\tau i)}. \tag{5}$$

When $f=0$ the low (zero) frequency limit of the susceptibility can be defined, $\chi_{\parallel l}^o=\gamma/\epsilon_0$, which gives the dependence of γ on the low frequency susceptibility $\gamma=\epsilon_0\chi_{\parallel l}^o$. We can then rewrite the orientational susceptibility (5) as

$$\chi_\parallel^o = \frac{\chi_{\parallel l}^o}{1+2\pi f\tau i}, \tag{6}$$

which is the commonly used Debye model of dielectric relaxation. The high frequency limit of the susceptibility is found by taking $f\to\infty$ which leads to $\chi_{\parallel h}^o=0$, in other words, at high frequencies the excitation of the parallel orientational polarization will relax and be $\mathbf{P}_\parallel^o=\mathbf{0}$.

Using Eqs. (1) and (6) we obtain the expression for the complete parallel susceptibility

$$\chi_\parallel = \chi_{\parallel l}^e + \frac{\chi_{\parallel l}^o}{1+2\pi f\tau i}. \tag{7}$$

From this expression we see that the low frequency susceptibility will be equal to $\chi_{\parallel l}^e+\chi_{\parallel l}^o$ and the susceptibility at high frequencies (but lower than the relaxation frequency of the electronic polarizations) will be approximately equal to $\chi_{\parallel l}^e$. In the direction perpendicular to the director, the measured susceptibility will be, from Eq. (1),

$$\chi_\perp = (\chi_{\perp l}^e + \chi_{\perp l}^o). \tag{8}$$

By experimentally exciting the parallel and perpendicular dielectrically induced polarizations, with an electric field of frequency f, we can use Eqs. (7) and (8), fitted to the experimental data, to find $\chi_{\parallel l}^{ea}, \chi_{\parallel l}^o$ (and therefore γ), τ and $\chi_\perp$. When we have determined these parameters we can consider a general electric field waveform using Eq. (3) to determine the parallel polarization and $\mathbf{P}_\perp=\chi_\perp\epsilon_0\mathbf{E}_\perp$ to determine the perpendicular polarization.

When calculating the dielectrically induced polarizations in a nonuniform sample care must be taken to ensure Maxwell's equations are also satisfied. In the present situation the displacement field is $\mathbf{D}=\epsilon_0\mathbf{E}+\mathbf{P}_\parallel+\mathbf{P}_\perp$ (for simplicity we have neglected flexoelectric polarization contributions). In the example we consider below we assume that the director lies in the xz plane so that we define the tilt angle θ such that $\mathbf{n}=(\cos\theta,0,\sin\theta)$. The displacement field in the z direction is then $D_z=\epsilon_0E_z+P_\parallel\sin\theta+P_\perp\cos\theta$, where $P_\parallel=|\mathbf{P}_\parallel|$, $P_\perp=|\mathbf{P}_\perp|$ and E_z is the component of the electric field in the z direction. In a system where variables only vary along one direction (which will be the z direction, perpendicular to the cell substrates in the example we consider below) we use the standard manipulation of the displacement field (see, for ex-

ample, Ref. [20,21]), together with Maxwell's equations $\nabla \cdot \mathbf{D}=0$ and $\nabla \times \mathbf{E}=\mathbf{0}$ to give the electric field in the z direction

$$E_z = \frac{V}{d} - \frac{1}{\epsilon_0}(P_\parallel \sin\theta + P_\perp \cos\theta) + \frac{1}{\epsilon_0 d}\int_0^d (P_\parallel \sin\theta + P_\perp \cos\theta)dz, \quad (9)$$

where $V=V(0)-V(d)$ is the potential difference applied between the two electrodes which are a distance d apart. The electric field components in the x and y directions may also be found and are equal to zero. The electrostatic free energy can then be written as

$$-\int \mathbf{D}d\mathbf{E} = -\left(\frac{1}{2}\epsilon_0 \mathbf{E}^2 + \mathbf{P}_\parallel \cdot \mathbf{E} + \mathbf{P}_\perp \cdot \mathbf{E}\right) = -E_z\left(\frac{1}{2}\epsilon_0 E_z + P_\parallel \sin\theta + P_\perp \cos\theta\right), \quad (10)$$

where $P_\parallel = P_\parallel^e + P_\parallel^o$ and $P_\perp = P_\perp^e + P_\perp^o$ and E_z is given by Eq. (9).

To model the director dynamics in response to the applied electric field we will assume that fluid flow effects are not important and only consider director rotation. This assumption is certainly not always the case and flow effects have been shown to be important in both experimental [10] and theoretical [22] investigations. However, for simplicity and to demonstrate the use of such a model we will neglect flow. Since electrostatic terms do not enter the governing equations for flow, the extension of the present model to incorporate flow is standard and can be found in [22] or derived fully in [21]. The governing equations for the director angle θ, the electric field in the z direction E_z, the electronic polarizations $P_\parallel^e, P_\perp^e$, and orientational polarizations $P_\parallel^o, P_\perp^o$ are therefore

$$\gamma_1 \frac{\partial\theta}{\partial t} = (K_1 \cos^2\theta + K_3 \sin^2\theta)\frac{\partial^2\theta}{\partial z^2} + \frac{1}{2}(K_3 - K_1)\sin\theta\cos\theta\left(\frac{\partial\theta}{\partial z}\right)^2 + [(P_\parallel^e + P_\parallel^o)\cos\theta - (P_\perp^e + P_\perp^o)\sin\theta]E_z, \quad (11)$$

$$E_z = \frac{V}{d} - \frac{1}{\epsilon_0}[(P_\parallel^e + P_\parallel^o)\sin\theta + (P_\perp^e + P_\perp^o)\cos\theta] + \frac{1}{\epsilon_0 d}\int_0^d (P_\parallel^e + P_\parallel^o)\sin\theta + (P_\perp^e + P_\perp^o)\cos\theta \mathrm{d}z, \quad (12)$$

$$P_\parallel^e = \chi_{\parallel l}^e \epsilon_0 E_z \sin\theta, \quad (13)$$

$$\tau\frac{dP_\parallel^o}{dt} = \epsilon_0 \chi_{\parallel l}^o E_z \sin\theta - P_\parallel^o, \quad (14)$$

$$P_\perp^e = \chi_{\perp l}^e \epsilon_0 E_z \cos\theta, \quad (15)$$

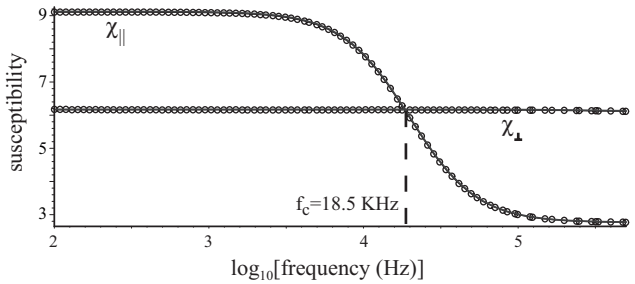

FIG. 1. Experimentally obtained susceptibility data (circles) and theoretical fit (solid lines) for $\chi_\parallel$ to the Debye equation (7) and the constant perpendicular susceptibility $\chi_\perp$ equation (8).

$$P_\perp^o = \chi_{\perp l}^o \epsilon_0 E_z \cos\theta, \quad (16)$$

where γ_1 is the rotational viscosity and K_1 and K_3 are the splay and bend elastic constants of the liquid crystalline material, respectively.

Equations (11)–(16) will be solved numerically using a simple Euler method to step forward in time. Spatial gradients are discretized using central differences. At each timestep the electric field is first calculated using Eq. (12) with variables taken from the previous timestep. The director equation (11) and polarization equations (13)–(16) are then solved explicitly using the updated electric field and other variables from the previous timestep. This simple numerical method is certainly not the most efficient or stable but, as long as care is taken in setting the length of time between timesteps, it is quick to implement, easy to ensure stability and gives sufficiently accurate results.

III. EXPERIMENTAL RESULTS

The susceptibilities $\chi_\parallel$ and $\chi_\perp$ were measured for the highly dispersive material MLC2048 (Merck) at 25 °C. The material was confined in a test cell of thickness 22 μm that consisted of a continuous electrode on one confining plate opposite to a circular electrode with an earthed guard ring on the opposite plate. For $\chi_\perp$ the cell surfaces were coated with a thin layer of a polymer that was rubbed parallel on both plates to give low pretilt planar alignment. For $\chi_\parallel$ the surfaces were coated with a thin layer of a polymer that gave homeotropic alignment. The complex susceptibilities were measured over a frequency range from 1000 Hz to 500 kHz using an Agilent 4284A LCR meter with an excitation voltage of 0.1 V r.m.s. The resulting susceptibility values are shown in Fig. 1. By fitting to the real part of the Debye equation (7), and the frequency independent Eq. (8), the parallel susceptibility characteristics and perpendicular susceptibility were found to be $\tau = 20.05 \times 10^{-6}$ s, $\chi_{\parallel l}^e = 2.77$, $\chi_{\parallel l}^o = 6.36$, and $\chi_\perp = 6.17$, see Fig. 1. The corresponding critical frequency, at which the parallel and perpendicular susceptibilities are equal, is $f_c = 18.53$ kHz.

Fredericksz transition measurements were carried out at the same temperature using the sample test cells and equipment described above. In Fig. 2 the experimental results for the planar and homeotropic alignment geometries are shown by the filled circles. The x axis shows the rms value of the ac

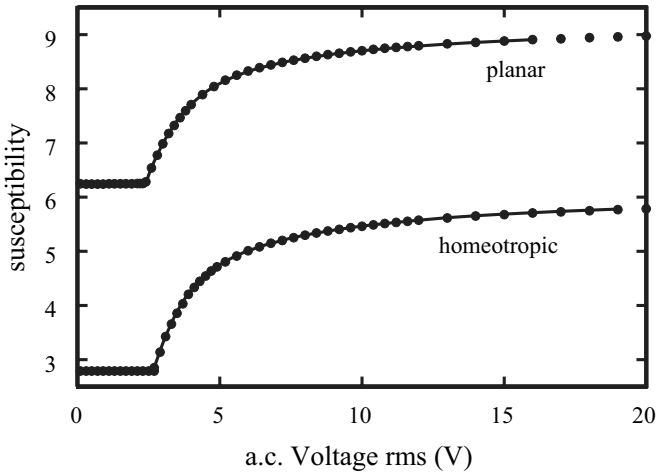

FIG. 2. Experimental measurements of the Fredericksz transition in the planar and homeotropic geometries. The filled circles show the experimental data and the continuous lines show the theoretical fit to the data using nematic continuum theory.

excitation voltage. The measurements in the planar geometry were performed with an excitation voltage of frequency 1000 Hz and a sharp Fredericksz threshold is observed at 2.5 V. Since the electric field is applied perpendicular to the cell substrates, the perpendicular component of the electric susceptibility $\chi_\perp=6.17$ is measured below this threshold. At 1000 Hz the electric susceptibility anisotropy is positive and so at high fields the susceptibility asymptotes towards the value $\chi^e_{\|l}+\chi^o_{\|l}$ as the director rotates in the bulk of the cell from planar alignment towards the homeotropic orientation.

The measurements in the homeotropic geometry were performed with an excitation voltage of frequency 500 kHz and a sharp Fredericksz threshold is observed at 2.7 V. Below this threshold the high frequency parallel component of the electric susceptibility, $\chi^e_{\|l}=2.77$, is measured. At 500 kHz the electric susceptibility anisotropy is now negative so at high fields the susceptibility asymptotes towards the value $\chi_\perp=6.17$ as the director rotates in the bulk of the cell from homeotropic alignment towards planar orientation.

From the value of the ac voltage at which the Fredericksz threshold occurred for each cell the elastic constants were found to be $K_1=15.8\times10^{-12}$ N and $K_3=21.8\times10^{-12}$ N. In addition to the measurements of the elastic constant values from the threshold it is also possible to fit the shape of the complete curve using nematic continuum theory. This gives the values $K_3/K_1=1.34$ and $K_1/K_3=0.69$ from the planar and homeotropic measurements, respectively. There is agreement to within 5% of the values for K_1 and K_3 derived from fitting the complete curve and the values derived from the Fredericksz thresholds. For the remainder of this paper the average of both results, $K_1=15.4\times10^{-12}$ N and $K_3=21.5\times10^{-12}$ N, have been used.

We do not have any data concerning the viscosity of this material so we have used $\gamma_1=0.05$ Pa s, a typical value for nematic liquid crystal materials [23], for the simulations reported in this paper. We further consider a cell of thickness $d=5\times10^{-6}$ m.

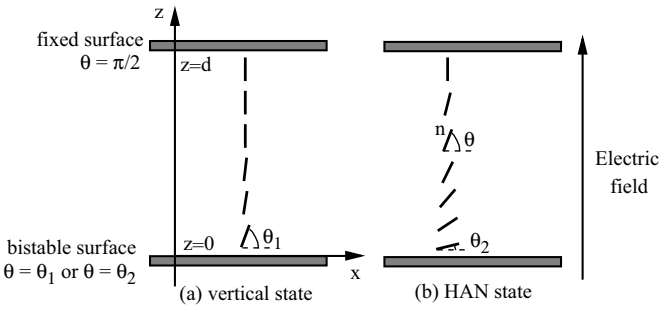

FIG. 3. Simple model of a zenithally bistable nematic cell. Due to bistable surface anchoring at the lower substrate, two states are possible, (a) the vertical and (b) the hybrid aligned nematic (HAN) states.

IV. THEORETICAL RESULTS

Using the above model and experimental parameters, we will now consider pulsed addressing of a simple model zenithally bistable nematic device, in which one surface allows two possible stable director positions, filled with a dual frequency material. This model cell, previously developed by Davidson and Mottram [24] as a model of a zenithally bistable nematic device such as the ZBD [25] or PABN [26] devices, considers a one-dimensional in-plane director configuration $\mathbf{n}(z)=[\cos\theta(z),0,\sin\theta(z)]$, where z is the coordinate perpendicular to the substrates and varies from 0 to d across the cell. To model the complicated two- or three- dimensional surface morphology of the ZBD or PABN devices a simple bistable surface anchoring energy is used to mimic the behavior of the substrate. We will use a simple surface energy which allows two possible surface alignments $\theta=\theta_1$ and $\theta=\theta_2$, see Fig. 3. Using this surface energy $(W/2)(\theta-\theta_1)^2(\theta-\theta_2)^2$, the calculus of variations leads to a balance of torques at the substrate. More details of this type of weak anchoring constraint are given in Ref. [21]. The second substrate is taken to exhibit infinitely strong homeotropic anchoring. The boundary conditions used to model these anchoring constraints are therefore

$$\frac{d\theta}{dz}=\frac{W(\theta-\theta_1)(\theta-\theta_2)(2\theta-\theta_1-\theta_2)}{(K_1\sin^2\theta+K_3\cos^2\theta)} \quad \text{at } z=0, \tag{17}$$

$$\theta=\pi/2 \quad \text{at } z=d, \tag{18}$$

where the bistable anchoring coefficient is taken to be $W=3\times10^{-5}$ N m^{-1} and the two director angles at which the bistable surface energy attains its minimum are $\theta_1=4\pi/9$ radians and $\theta_2=\pi/18$ radians. There are therefore two possible stable director configurations, a state in which the director is largely in the z direction throughout the cell (called the vertical state here) and a state in which the director angle varies from homeotropic at the upper surface to close to the θ_2 value at the lower surface [called the hybrid aligned nematic (HAN) state here], see Fig. 3. Switching between the two states has been shown to be possible using flexoelectric effects [24] but we will show that this is also possible without the use of flexoelectric coupling but with a dual

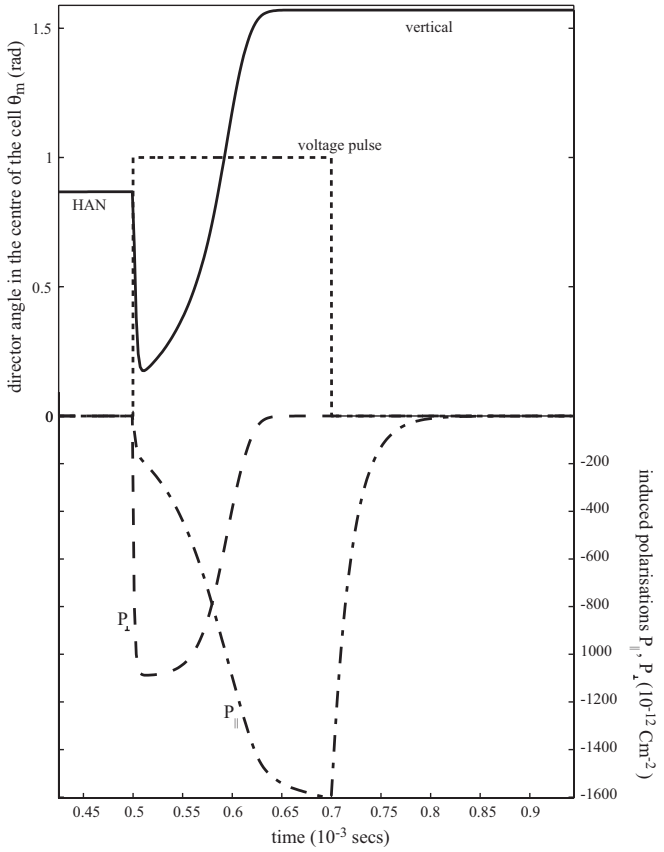

FIG. 4. Simulated response to a voltage pulse of height 100 V and length 0.2 ms. The director angle at the middle of the cell ($z=d/2$) is plotted (solid line) together with the parallel (dash-dotted line) and perpendicular (dashed line) induced polarizations. The voltage pulse (dotted line) is also plotted, scaled by the height of the pulse, for reference.

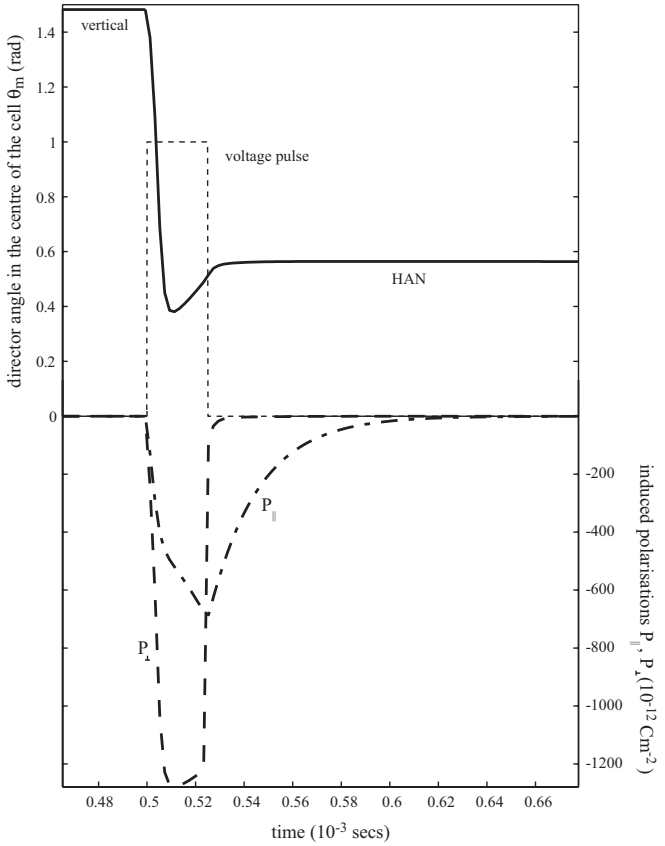

FIG. 5. Simulated response to a voltage pulse of height 125 V and length 0.025 ms. The director angle at the middle of the cell ($z=d/2$) is plotted (solid line) together with the parallel (dash-dotted line) and perpendicular (dashed line) induced polarizations. The voltage pulse (dotted line) is also plotted, scaled by the height of the pulse, for reference.

frequency material. Such switching is easy to envisage if a sinusoidal voltage waveform is employed. For applied voltages of low frequencies the material behaves as a positive dielectric material and molecules will tend to align in the field direction causing the vertical state to be attained. For a high frequency voltage waveform ($f>f_c$) the material will behave as a negative dielectric material, the director will tend to lie parallel to the substrates, except close to the strongly anchored upper surface, and the HAN state will be attained. However, since the use of sinusoidal voltage waveforms is not practical in display devices, we aim to show that pulsed rather than sinusoidal voltages can achieve the same effect.

Figures 4 and 5 show the simulated director orientation at the center of the cell, θ_m (at $z=d/2$), when different voltage pulses are applied to the cell. For Fig. 4 the system was started in the HAN state and a voltage pulse of height 100 V was applied for 0.2 ms (after an initial period of 0.5 ms during which the system equilibriates). For Fig. 5 the system was started in the vertical state and a voltage pulse of height 125 V was applied for 0.025 ms. We see that using the long pulse (Fig. 4) it is possible to switch from a HAN state to a vertical state and using a shorter pulse, of a higher voltage, it is possible to switch from a vertical state to a HAN state. In Figs. 4 and 5 we have also plotted the calculated polarizations parallel and perpendicular to the nematic director $P_{\|}$ and $P_{\perp}$, respectively. In Fig. 4 we see that the parallel polarization is slow to react to the applied voltage so that the perpendicular polarization becomes larger in magnitude than the parallel polarization for a short time after the voltage is applied. This will cause an effective negative dielectric anisotropy and the director will tend to align perpendicular to the electric field, consequently θ_m reduces. However, eventually, while the voltage remains on, the parallel polarization becomes larger than the perpendicular polarization causing an effective positive dielectric anisotropy and inducing an increase of the director angle so that the cell is switched into the vertical state. In Fig. 5 we see that when the voltage is removed before the magnitude of the parallel polarization has time to increase above the perpendicular polarizing the director remains perpendicular to the field and the cell can be switched into the HAN state.

We can now study the switching characteristics for a range of voltage pulse heights and lengths in the following way: The theoretical system was initially set in one of the equilibrium states (vertical or HAN) and the voltage pulse was applied. A sufficient length of time was allowed after the

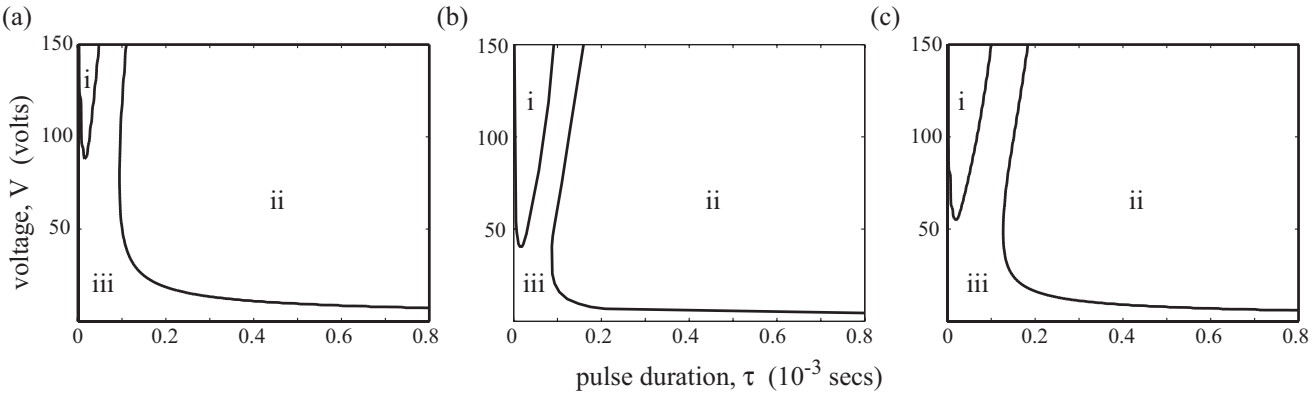

FIG. 6. Switching regimes for voltage pulses of duration τ and peak voltage V for parameter values given in the text except in (b) where $\gamma_1=0.01$Pa s and (c) where $\chi^e_{\|l}=5$, $\chi^o_{\|l}=15$, and $\chi_\perp=15$. In region (i) the vertical state switches to the HAN state, in (ii) the HAN state switches to the vertical state, and in region (iii) no switching between states occurs.

pulse to ensure the director configuration had then reached equilibrium. The pulse lengths and pulse voltages which induced switching were then recorded. Using voltage waveforms between 0 and 150 V and of pulse lengths between 0 and 0.8 ms the voltage waveforms which induced switching were recorded and are presented in Fig. 6(a). We see that short pulses, of high enough voltage, cause the system to switch to the HAN state. As explained above, in this case the high frequency components of the leading edge of the voltage pulse excites the perpendicular polarization and forces the director to lie parallel to the cell substrates. For longer pulses, switching to the vertical state is possible since the constant dc component of the voltage pulse excites the parallel polarization causing the director to lie perpendicular to the substrates.

For these parameter values, we have found that switching to the HAN state only occurs at relatively high voltages (certainly compared to those required for standard liquid crystal devices); we have also, however, modeled two alternative (hypothetical) liquid crystal materials, one in which the rotational viscosity has been reduced, to $\gamma_1=0.01$ Pa s, and one in which the high frequency dielectric anisotropy is larger, $\chi^e_{\|l}=5$, $\chi^o_{\|l}=15$, and $\chi_\perp=15$ to enable a greater response to the electric field from the perpendicular polarization. The results for these two materials are shown in Figs. 6(b) and 6(c). In both cases the vertical to HAN state switching region has extended to lower voltages and larger pulse durations.

V. CONCLUSIONS

We have presented a theoretical model of dielectric relaxation in order to model the response of dual frequency materials to arbitrary waveforms. The equations governing the director angle, electric field, and induced polarizations are then solved numerically to investigate voltage pulse addressing of a model zenithally bistable liquid crystal device. We find that, by suitably tailoring the voltage pulse, it is possible to switch between both bistable states. For short pulses the high frequency components of the leading edge of the voltage pulse excite the perpendicular polarization and force the director to lie parallel to the substrates, enabling switching to the HAN state. For long voltage pulses the constant dc component of the voltage pulse will excite the parallel polarization and cause the director to lie perpendicular to the substrates, enabling switching to the vertical state. We have also shown that reducing rotational viscosity and increasing the achievable dielectric anisotropies (particularly the high frequency value) can significantly reduce the operating voltages of such a device. It is hoped that an experimental investigation on a ZBD or PABN cell filled with a dual frequency material will be able to verify these predictions.

ACKNOWLEDGMENTS

The authors wish to thank Dr S.A. Jewell and Professor J.R. Sambles for instigating this work as well as Drs M. Francis and M. Goulding of Merck NB-C Southampton for the experimental test cells and the material.

[1] P. Debye, in *Polare Molekeln* (Hirzel Verlag, Leipzig, 1929).
[2] W. Maier and A. Saupe, Z. Naturforsch. A **15**, 287 (1960).
[3] W. Maier and G. Meier, Z. Naturforsch. A **16**, 262 (1961).
[4] A. J. Martin, G. Meier and A. Saupe, Symp. Faraday Soc. **5**, 119 (1971).
[5] H. Kresse, in *Physical Properties of Liquid Crystals: Nematics*, edited by D. A. Dunmur, A. Fukuda, and G. R. Luckhurst (IEE, London, 2001).
[6] W. Haase and S. Wróbel, *Relaxation Phenomena: Liquid Crystals, Magnetic Systems, Polymers, High-T_C Superconductors, Metallic Glasses* (Springer Verlag, Berlin, 2003).
[7] M. Schadt, Mol. Cryst. Liq. Cryst. **66**, 319 (1981).
[8] M. Schadt, Mol. Cryst. Liq. Cryst. **89**, 77 (1982).
[9] E. P. Raynes and I. Shanks, Electron. Lett. **10**, 114 (1974).
[10] M. G. Clark, in *Non-linear Phenomena and Chaos*, edited by S. Sarkar (Adam Hilger, Bristol, 1986).

[11] S. A. Jewell and J. R. Sambles, Opt. Express **13**, 2627 (2005).
[12] T. Kuki, H. Fujikake, and T. Nomoto, IEEE Trans. Microwave Theory Tech. **50**, 2604 (2002).
[13] D. Dayton, S. Browne, J. Gonglewski, and S. Restaino, Appl. Opt. **40**, 2345 (2001).
[14] Y.-Q. Lu, X. Liang, Y.-H. Wu, F. Du, and S.-T. Wu, Appl. Phys. Lett. **85**, 3354 (2004).
[15] S. R. Restaino, D. Dayton, S. Browne, J. Gonglewski, J. Baker, S. Rogers, S. McDermott, J. Gallegos, and M. Shilko, Opt. Express **6**, 2 (2000).
[16] R. J. Turnbull, J. Phys. D **6**, 1745 (1973).
[17] M. Felczak and G. Derfel, Liq. Cryst. **30**, 739 (2003).
[18] I. R. Guralnik, V. N. Belopukhov, G. D. Love, and A. F. Naumov, J. Appl. Phys. **87**, 4069 (2000).
[19] P. G. de Gennes and J. Prost, *The Physics of Liquid Crystals* (Oxford University Press, Oxford, 1994).
[20] M. J. Towler, J. R. Highes, and F. C. Saunders, Ferroelectrics **113**, 453 (1991).
[21] I. W. Stewart, *The Static and Dynamic Continuum Theory of Liquid Crystals* (Taylor and Francis, London, 2004).
[22] P. D. Brimicombe, L. A. Parry-Jones, S. J. Elston, and E. P. Raynes, J. Appl. Phys. **98**, 104104 (2005).
[23] V. V. Belyaev, in *Physical Properties of Liquid Crystals: Nematics*, edited by D. A. Dunmur, A. Fukuda, and G. R. Luckhurst (IEE, London, 2001).
[24] A. J. Davidson and N. J. Mottram, Phys. Rev. E **65**, 051710 (2002).
[25] G. P. Bryan-Brown, C. V. Brown, and J. C. Jones, Patent GB 95521106.6 (unpublished).
[26] C. J. P. Newton and T. P. Spiller (unpublished).